

Electromagnetic production of kaons

R. A. Adelseck and L. E. Wright

Physics Department, Ohio University, Athens, Ohio 45701

(Received 25 July 1988)

Employing diagrammatic techniques, a model for the reactions ${}^1\text{H}(\gamma, K^+)\Lambda$ and ${}^1\text{H}(e, e'K^+)\Lambda$ is derived with the coupling constants being determined phenomenologically by a least-squares fit to the available data. We find a strong sensitivity of the photoproduction process to t -channel exchange terms. The inclusion of the kaon resonance $Q1(1280 \text{ MeV})$ brings the dominant $K\Lambda N$ coupling constant in agreement with predictions from the analysis of Kp scattering data. An excellent fit to the electroproduction data confirms former measurements of the kaon radius.

The production of strange particles has become of significant concern due to the rapid development of hypernuclear physics. In order to extract sensitive information from the study of hypernuclei, we are confronted with the need for a well-understood production mechanism. Thus we consider an electromagnetic probe in the initial state, creating the relatively weakly interacting K^+ associated with the hyperon in the final state. The high photon energy, i.e., short wavelength, needed to reach the regime of kaon production justifies an impulse approximation based on the elementary processes ${}^1\text{H}(\gamma, K^+)\Lambda$ or ${}^1\text{H}(\gamma, K^+)\Lambda$. Phenomenological models for the kaon photoproduction process have been derived by many groups,¹⁻⁴ but to date no analysis of the reaction ${}^1\text{H}(e, e'K^+)\Lambda$ has been made. Moreover, the results from the photoproduction analysis remain questionable⁵ due to inconsistencies in the value of the dominant $K\Lambda N$ coupling constant when compared to independent determinations from hadronic processes^{6,7} or quark model calculations.⁸ Presently, the strength of the $K\Lambda N$ coupling as determined from electromagnetic interactions reaches at most half of the value as implied by processes involving the strong interaction. For comparison, we show a representative list of determinations of the $K\Lambda N$ coupling in Table I.

We derive the scattering amplitude for the elementary process ${}^1\text{H}(e, e'K^+)\Lambda$ in the framework of the one-photon exchange approximation, given by

$$T = \epsilon_\mu \cdot J^\mu,$$

TABLE I. Numerical value of $K\Lambda N$ coupling constant ($g_\Lambda/\sqrt{4\pi}$) as determined from electromagnetic (EM) and hadronic (H) processes, and quark model calculations (Q).

Type	Reference	Value
EM	1	2.0
EM	2	2.49
H	9	2.43
H	6	4.62
H	7	3.73
Q	8	4.13
EM	3	1.29
EM	4	0.92
EM	Present work	4.30

where μ runs from 0 to 3. The polarization four-vector ϵ_μ of the virtual photon is directly related to the electron current:

$$\epsilon_\mu = \bar{u}(\mathbf{p}_{e'}) \gamma_\mu u(\mathbf{p}_e) / p_\gamma^2,$$

with the photon's four-momentum being denoted by $p_\gamma = p_{e'} - p_e$.

In a preceding study,³ we have calculated the amplitude describing the hadronic current J^μ by means of Feynman diagrams for the Born terms (p , Λ , K^+ , Σ , and K^* exchange), as well as for resonant states in the s (N^*), t (K^*), and u channel (Y^*). All diagrams are shown in Fig. 1 of that reference. In addition to the resonances shown in Table II of Ref. 3, we investigate the effects of a second kaon resonance (the pseudovector state $Q1$ with a mass of 1280 MeV, a width of 90 MeV), and two more u -channel resonances ($J^\pi = \frac{1}{2}^+$, $M = 1600 \text{ MeV}$, $\Gamma = 150 \text{ MeV}$, and $J^\pi = \frac{1}{2}^+$, $M = 1800 \text{ MeV}$, $\Gamma = 150 \text{ MeV}$).

For virtual photons, the transition matrix T can be covariantly expressed in terms of six Lorentz and gauge invariant amplitudes A_i :

$$T = \bar{u}(\mathbf{p}_\Lambda) \sum_{i=1}^6 A_i M_i u(\mathbf{p}_n),$$

where M_i are six known Lorentz-invariant matrices,¹⁰ rather than four matrices as in the case of real photons.

The coupling constants are obtained by a least-squares fit to (a) all available photoproduction data,¹¹ (b) electroproduction data¹²⁻¹⁵ and (c) both sets. We also compare the sensitivity of the operator to various resonances. The best fit was obtained after including the $N1$, $N4$, Σ^0 , $Y2$, K^* , and $Q1$ resonances. A list of all coupling constants is given in Table II. Sets I and II were obtained by fitting photoproduction data up to 1.4 GeV photon energy, while set III employed the electroproduction data and set IV used both data sets. The nomenclature of the coupling constants follows Ref. 3; the coupling of $Q1$ is chosen analogous to the vector-kaon coupling, the only differences being its opposite parity resulting in an additional γ_5 factor. Note that the secondary coupling constants vary considerably from fit to fit. The processes being investigated with the currently available data cannot claim to determine their individual values, but rather the set of values are determined. Individually, the terms involving

TABLE II. Effective coupling constants for ${}^1\text{H}(\gamma, K^+)\Lambda$ (sets I, II), ${}^1\text{H}(e, e'K^+)\Lambda$ (set III), and the combined data set (set IV).

Set	I	II	III	IV
$g_{\Lambda}/\sqrt{4\pi}$	2.40	4.30	2.90	3.15
$G_{\Sigma}/\sqrt{4\pi}$	0.0951	3.60	6.73	3.28
$G_{\nu}/r\pi$	0.121	0.124	-0.0203	0.0279
$G_{\tau}/4\pi$	-0.0135	-0.338	-0.188	-0.188
$G_{N1}/\sqrt{4\pi}$		-0.907	-4.49	-1.11
$G_{N2}/\sqrt{r}\pi$		0.103	0.540	0.101
$G_{\nu 3}/\sqrt{4\pi}$		3.35	-0.285	0.698
$G_{\rho}^0/4\pi$		0.269	0.0959	0.132
$G_{\rho}^{\pm}/4\pi$		0.829	0.123	0.0630
χ^2/N	8.722	4.903	2.247	3.723

the secondary coupling constants do not play a dominant role.

We found that the coupling constants for ${}^1\text{H}(\gamma, K^+)\Lambda$ were not very well determined, being very susceptible to changes in the available data set. We consider this as evidence for inconsistencies hidden in the photoproduction data. However, by including the $Q1$ t -channel resonance, the dominant $K\Lambda N$ coupling showed a general increase in strength, suggesting that $Q1$ provides a necessary contribution to the photoproduction process. Rosenthal *et al.*⁴ recently investigated the effect of a spin-2 tensor resonance in the t channel, but found little improvement in the fit. Moreover, their $K\Lambda N$ coupling dropped to a value less than 1. A comparison of the differential cross section as predicted by sets I, II, and IV to some of the data is shown in Fig. 1. Through the addition of the $Q1$ resonance, we are able to reproduce the proper angular distribution.

Our analysis of the reaction ${}^1\text{H}(e, e'K^+)\Lambda$ revealed an extremely consistent data set. The $K^+\Lambda N$ coupling constant varied only from 2.84 for using the "true" Born terms ($p-$, $\Lambda-$, and K^+ exchange only) to 2.90 with all resonances mentioned above being included. The corresponding χ^2 per degree of freedom changed from 5.273

(24.76 for photoproduction) to 2.247. The fit was very sensitive to the choice of the mass parameter in the kaon form factor, for which we adopted the vector dominance model. We found a strong preference for a mass parameter of 950 MeV which is equivalent to a kaon radius of 0.51 fm. Hsiao and Cotanch¹⁶ were only able to reproduce the electroproduction cross section under the assumption of an unphysically small kaon size due to their use of Thom's coupling constants. Our result confirms earlier direct measurements done by electron scattering.¹⁷ For the lambda we employed the same form factor as for the neutron, apart from using the appropriate mass. The $K\Lambda N$ coupling constant is somewhat lower than in the case of (γ, K^+) , but by dividing out the $\Lambda - \Sigma$ transition moment [$-1.82\mu_N$ (Ref. 18)] we obtain an effective $K\Lambda N - k\Sigma N$ coupling of 16.1 in agreement with determinations^{7,19} from hadronic interactions. Figure 2 compares the predictions of sets II, III, and IV with measurements from the ${}^1\text{H}(e, e'K^+)\Lambda$ reaction.¹⁴ The disagreement of set I with the data points can be understood by the relatively high equivalent photon energy of 2.2 GeV, which is beyond our photoproduction fit. The agreement of set III with the data is remarkable, and even set IV provides a rather good description of the process.

It appears that the electroproduction process, though at much higher energies than the investigated photoproduction process, is very well described by a few selected first-order Feynman diagrams. The quality of the $(e, e'K^+)$ data set seems to be of a higher standard than the (γ, K^+) data, suggesting the need for improved measurements of the photoproduction process.

The reaction ${}^1\text{H}(\gamma, K^+)\Lambda$ displays a critical dependence on t -channel resonances. Inclusion of the $Q1$ resonant state of the kaon resolves inconsistencies in the numerical value of the primary $K^+\Lambda N$ coupling constant encountered when using electromagnetic instead of hadronic probes.

We suggest that set II provides an adequate description

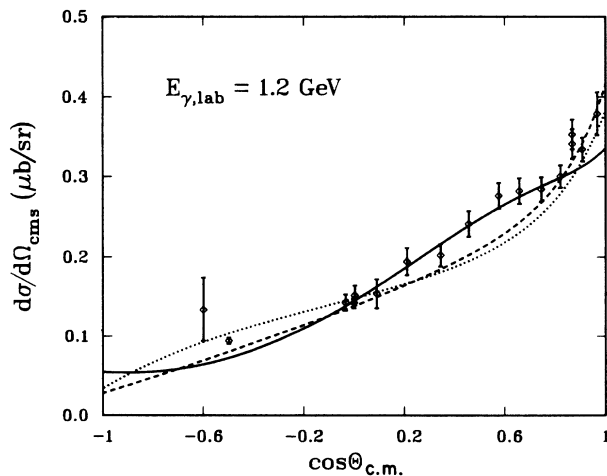


FIG. 1. Angular distribution of ${}^1\text{H}(\gamma, K^+)\Lambda$. The dotted curve represents set I, the dashed curve employs set IV and the solid curve shows our best fit given by set II.

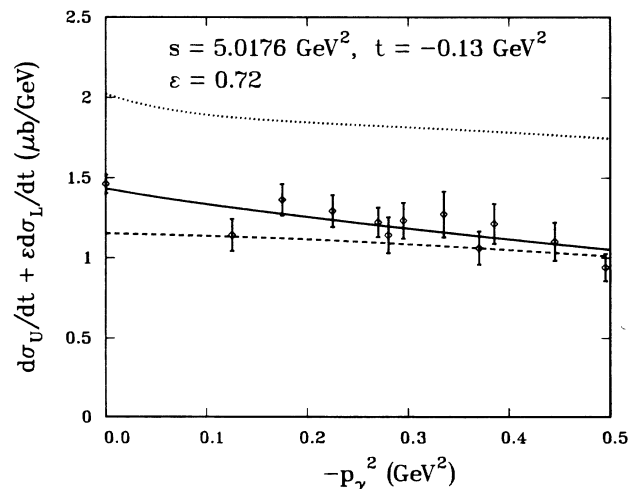


FIG. 2. Cross section for ${}^1\text{H}(e, e'K^+)\Lambda$. The solid curve is a prediction of our best fit (set III), the dotted curve is an extrapolation of the photoproduction operator (set II), and the dashed curve represents a fit to all data (set IV).

of the reaction ${}^1\text{H}(\gamma, K^+)\Lambda$, while set III proves to be the appropriate model for ${}^1\text{H}(e, e'K^+)\Lambda$. Further measurements, in particular of the photoproduction process, are urgently needed in order to clarify the inconsistencies encountered in the currently available data. More precise data in a wider energy range might also be able to remove the small discrepancies between real and virtual photoproduction of kaons.

This good description of the elementary process provides a firm basis for predicting kaon production cross sections from nuclei and, once these experiments can be per-

formed on the new generation of electron accelerators, the extraction of information on hypernuclear structure and hyperon wave functions. Conversely, it is feasible, with a given hypernuclear structure, to obtain more details on the elementary process since certain pieces of the basic operator can be selected and enhanced by an appropriate choice of the initial and final nuclear states.

This work was supported in part by U.S. Department of Energy Grant No. DE-FG02-87ER40370.

¹T. K. Kuo, Phys. Rev. **129**, 2264 (1963).

²H. Thom, Phys. Rev. **151**, 1322 (1966).

³R. A. Adelseck, C. Bennhold, and L. E. Wright, Phys. Rev. C **32**, 1681 (1985).

⁴A. S. Rosenthal *et al.*, Ann. Phys. (N.Y.) **184**, 33 (1988).

⁵Joseph Cohen, Phys. Rev. C **37**, 187 (1988).

⁶Carl B. Dover and George E. Walker, Phys. Rep. **89**, 1 (1982).

⁷O. Dumbrajs *et al.*, Nucl. Phys. **B216**, 277 (1983).

⁸M. Bozoian *et al.*, Phys. Lett. **122B**, 138 (1983).

⁹Ya. I. Granovskii and V. N. Starikov, Yad. Fiz. **6**, 610 (1966) [Sov. J. Nucl. Phys. **6**, 444 (1967)].

¹⁰E. Amaldi, S. Fubini, and G. Furlan, *Pion-Electroproduction* (Springer, Berlin, 1979).

¹¹*Landolt-Börnstein: Numerical Data and Functional Relationships in Science and Technology* (Springer, New York, 1973), Vol. 8.

¹²C. N. Brown *et al.*, Phys. Rev. Lett. **28**, 1086 (1972).

¹³C. J. Bebek *et al.*, Phys. Rev. Lett. **32**, 21 (1974); Phys. Rev. D **15**, 594 (1977); *ibid.* **15**, 3082 (1977).

¹⁴T. Azemoon *et al.*, Nucl. Phys. **B95**, 77 (1975).

¹⁵P. Brauel *et al.*, Z. Phys. C **3**, 101 (1979).

¹⁶Shian S. Hsiao and Stephen R. Cotanch, Phys. Lett. **163B**, 300 (1985).

¹⁷E. B. Dally *et al.*, Phys. Rev. Lett. **45**, 232 (1980).

¹⁸F. Dydak *et al.*, Nucl. Phys. **B216**, 1 (1977).

¹⁹A. D. Martin, Nucl. Phys. **B179**, 33 (1981).